Unmanned Systems, Vol. 14, No. 1 (2026) 157–166

DOI: 10.1142/S2301385025500888

Unmanned Systems
https://www.worldscientific.com/worldscinet/us

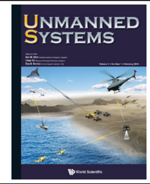

Performance of Airfoil Plunging Using Sinusoidal Waves Superposition

Mostafa El-Salamony

Institute of Aviation Engineering and Technology,
Cairo, Egypt

State Key Laboratory of Turbulence and Complex Systems,
Collaborative Innovation Center of Advanced Aero-Engine,
Peking University, Beijing 100871, China

This paper aims to study the aerodynamic and propulsive performance of a plunging airfoil using novel plunging waveform, that creates additional trailing edge vortices, that affects the flow field and, consequently, the aerodynamic loads on the airfoil. This waveform is generated by means of superpositioning of the regular sinusoidal wave with a faster one. This novel waveform not only allows to add another pair of trailing edge vortices but also to control their strength. It is found that as the weight of the faster wave increases, the thrust coefficient increases rapidly while the propulsive efficiency decreases slowly, allowing a window of high thrust with small efficiency reduction. Understanding the effect of generating additional trailing edge vortices within the regular flapping cycle on the propulsive performance is the main objective of this work.

Keywords: Unsteady aerodynamics; plunging; flapping; vortex structure; fluid–structure interaction.

1. Introduction

Unmanned Aerial Vehicles (UAVs), more commonly known as drones, have seen a significant increase in their applications, ranging from surveillance to delivery services. A specific type of UAVs that employ flapping wings for flight, mimicking the flight mechanics of birds and insects, have gained considerable interest [1, 2]. The study of the forces on flapping wings is of paramount importance in the field of UAVs. Not only it aids in understanding and improving the flight mechanics of these vehicles but also paves the way for innovative design and control strategies inspired by nature. As the demand for efficient and versatile UAVs continues to grow, the significance of studying the forces on flapping wings will also increase. One primary reason for studying the forces on flapping wings is to understand the flight mechanics of these UAVs [3]. The forces acting on the wings during the flapping cycle, which include lift, drag/thrust, determine the flight characteristics of the UAV. By studying these forces, we can gain insights into the stability, maneuverability and efficiency of the UAV. Analyzing the forces on flapping wings can aid in the design optimization of these UAVs [4]. By understanding how different design parameters such as wing shape, size, and flapping frequency affect the forces on the wings, we can optimize these parameters to improve the performance of the UAV. For instance, we might be able to design wings that generate more lift or reduce drag, thereby increasing the payload capacity or energy efficiency of the UAV [5].

The forces on flapping wings are also essential for developing control algorithms for these UAVs [6, 7]. These algorithms need to account for the time variation of the forces on the wings to accurately control the UAVs flight. For example, by knowing the lift force generated by the wings, the control algorithm can determine how much to flap the wings to achieve a desired altitude for a given payload, or the flapping power during sudden change in its weight.

Received 20 January 2024; Accepted 1 November 2024; Published 7 December 2024. This paper was recommended for publication in its revised form by editorial board member, H. T. Liu.
Email Address: *cblee@mech.pku.edu.cn*

The study of forces on flapping wings is also crucial for structural analysis of these UAVs. The wings of a UAV are subjected to various forces during flight, including aerodynamic forces due to air flow, inertial forces due to acceleration, and gravitational forces. These forces can induce stresses and strains in the wing material, which can lead to deformation or even failure of the wing structure. By studying these forces, we can predict the structural response of the wings under different flight conditions and ensure that the wings have sufficient strength and stiffness to withstand these forces [8]. This can help in preventing structural failures, improving the reliability and safety of the UAVs.

The forces on flapping wings also have significant implications for the design of flapping mechanisms. The flapping mechanism is the component of the UAV that generates the flapping motion of the wings. The design of this mechanism needs to account for the forces on the wings to ensure that it can generate the required flapping motion without failure. Moreover, the forces on the wings can affect the power requirements of the flapping mechanism. By studying these forces, we can design more efficient flapping mechanisms that minimize power consumption, thereby extending the flight duration of the UAVs [9, 10].

Finally, studying the forces on flapping wings can provide biomimetic insights, i.e. understanding how birds and insects fly and applying these principles to improve the design and control of flapping wing UAVs [11]. This biomimetic approach has the potential to lead to innovative solutions that enhance the performance of these UAVs beyond what is achievable with traditional aeronautical engineering approaches.

In [12], they focused on the effects of nonsinusoidal heaving trajectory, nonsinusoidal pitching trajectory, and the effective angle of attack on the energy extraction performances of a flapping foil operating at low Reynolds number ($\mathrm{Re} = 1100$). The study found that the best propulsive efficiency is obtained for sinusoidal paths, while nonsinusoidal ones are found to slightly improve thrust and lift forces.

The effect of nonsinusoidal trajectory on the propulsive performances and the vortex shedding process behind a flapping airfoil was investigated in [13]. A movement of a rigid NACA0012 airfoil undergoing a combined heaving and pitching motions at low Reynolds number ($\mathrm{Re} = 11{,}000$) was considered. Although the maximum propulsive efficiency is always achievable with sinusoidal kinematics, nonsinusoidal kinematics are found to considerably improve performance: A 110% increase of the thrust force was obtained in the best studied case.

Another study [14] found that when the pitching amplitude was small, the trapezoidal pitching profile could indeed improve the mean output power coefficient of the flapping foil. However, when the pitching amplitude was larger than the optimal value, the nonsinusoidal pitching motion negatively contributed to the propulsion performance.

Aim of this study is to quantify the aerodynamic and propulsive performance of a plunging airfoil using two-peak waveform kinematics. Superposition of fast and slow sinusoidal waves creates four inflection points per cycle, that generates additional Trailing Edge Vortices (TEVs) that affects the flow field and, consequently, the aerodynamic loads on the airfoil. The aerodynamic performance of the proposed waveform is studied on a plunging NACA 0012 airfoil in terms of lift, thrust and power coefficients and propulsive efficiency. Then, it is followed by a comparison with the performance using regular sinusoidal waveform plunging with the same flight and plunging characteristics to quantify the new waveform performance. The benefits are quantified by means of creating regression models for each performance parameter. Also, the time variation of the coefficients are presented. The paper is structured as follows. The study methodology is stated in Sec. 2 and the resultant aerodynamic and propulsive performance is discussed in Sec. 3, followed by a comparison between the performance of the proposed waveform and the sinusoidal one using regression modeling in Sec. 4, and the work is concluded in Sec. 5. Understanding the effect of generating a second TEV within the regular flapping cycle, and is effect on the propulsive performance is the main objective of this paper.

2. Methodology and Problem Formulation

2.1. *Plunging kinematics and the proposed waveform*

Plunging motion refers to the vertical motion of the entire airfoil parallel to the flow direction. This motion can be described as a periodic upward and downward translation of the airfoil. In fluid mechanics, plunging motion affects the flow structure by causing changes in the effective angle of attack, resulting in variations in lift and drag forces. Most of studies implement a sinusoidal motion in the vertical direction as

$$y(t) = A \times \sin(2\pi f t), \tag{1}$$

where $y(t)$ is the vertical position of the airfoil, A is the motion maximum amplitude in meters, and f is the dimensional frequency of the plunging motion, in Hertz.

In this study, a new waveform is proposed, in which it is formed from a superposition between the main sinusoidal wave and a N-times faster sinusoidal one and weighted by the parameter α. In the present case, the fast wave has a three times faster frequency and the weighting parameter

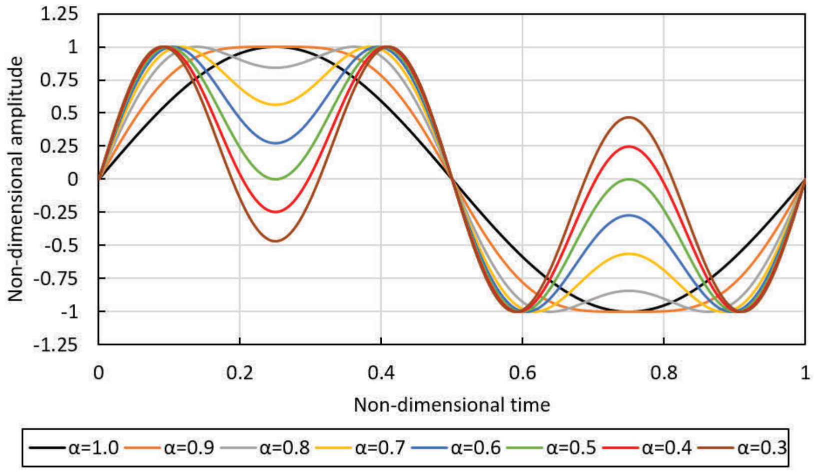

Fig. 1. Waveforms of the plunging motion for different values of the weighting parameter α.

varies from 1.0 to 0.3, as shown in Eq. (2). Figure 1 shows the family of studied waveforms side by side with the regular sine waveform for the means of comparison. The time and amplitude in this figure are nondimensionalized based on the periodic time of the flapping cycle and the plunging maximum amplitude, respectively, and all waves have the same periodic time and peak-to-peak amplitude. It shall be noted that when α is set to unity, the equation returns to Eq. (1).

$$y(t) = A[\alpha \sin(2\pi ft) + (1-\alpha)\sin(N \times 2\pi ft)]. \quad (2)$$

Since this proposed waveform is obtained from two sinusoidal waves, then this composite waveform is sinusoidal, continuous, harmonic and differentiable up to any order. By making the function smooth we overcome the issue of getting undefined values of velocity or acceleration naturally without need of additional smoothing or complicated blending functions. These features lead to simpler implementation in terms of the mechanical design of the flapping system [15].

A unique feature of this proposed waveform is the presence of two peaks each half cycle, with smooth transition between them, governed by the weighting factor α where it varies from 1.0 (pure sine) to 0.3. This allows us to understand clearly the effect of generating a second TEV within the regular flapping cycle, and its effect on the propulsive performance.

2.2. *Problem formulation*

NACA 0012 airfoil undergoing pure plunging motion is studied in the numerical analysis. The nondimensional plunging amplitude (h) and reduced frequency (k) are defined in Eqs. (3) and (4), respectively, as follows:

$$h = A/C, \quad (3)$$

$$k = \frac{2\pi fC}{U_o}, \quad (4)$$

where C is the airfoil chord, f is the plunging frequency and U_o is the free stream velocity. Reynolds number is defined based on the free stream velocity and chord as the characteristic speed and length scales.

For the h and k combination used, the instantaneous and time-averaged lift, thrust and power coefficients and the propulsive efficiency parameters are calculated according to:

$$\bar{C_T} = -\frac{1}{T}\int_t^{t+T} C_D(T)dt, \quad (5)$$

$$\bar{C_P} = -\frac{1}{TU_o}\int_t^{t+T} C_L(T)\dot{y}(T)dt, \quad (6)$$

$$\eta_P = \frac{\bar{C_T}}{\bar{C_P}}, \quad (7)$$

where $\bar{C_T}$ and $\bar{C_P}$ are the time average thrust and power coefficients, $C_D(t)$ and $C_L(t)$ are the instantaneous drag and lift coefficients, T is time period in seconds, $\dot{y}(T)$ is the plunging velocity, and η_P is the propulsive efficiency. All the parameters and definitions follow the standard ones mentioned in [16].

2.3. *Computational setup*

A plunging NACA 0012 airfoil with 10-cm chord at zero angle of attack is simulated using ANSYS CFX 18. The airfoil is treated as a moving boundary inside the domain and

Mesh Deformation technique is adopted. The Reynolds number is set to be 20,000, which makes the far field velocity is 3.09 m/s. The results of this value of Reynolds number is qualitatively similar to a wide range of Reynolds numbers [17]. The airfoil is plunging with nondimensional peak-to-peak amplitude of 0.15 and reduced frequency of 4, corresponding to 0.015 m and 19.67 Hz in the dimensional form. For this simulation SST turbulence model is utilized. Both CFL and Y+ are in order of unity in all cases.

The domain size is studied to ensure that the numerical results are least dependent on the boundaries. The domain height varies from 10 to 18 chord lengths and the domain width is changed from 11 to 23 chord lengths. It is shown that the lift coefficient change is within 2% in both cases, as shown in Fig. 2.

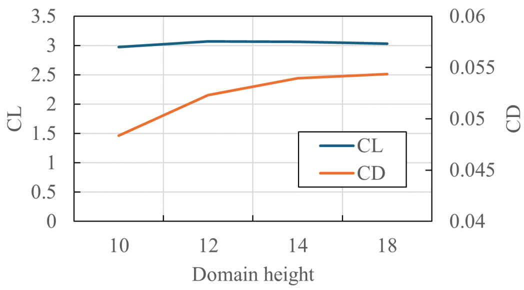

(a)

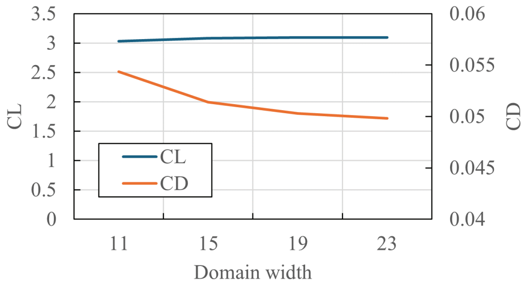

(b)

Fig. 2. Lift and drag coefficients variation with domain (a) height and (b) width.

The domain is selected to be a rectangle with dimensions of 21 C width and 20 C height and the airfoil is located at the center, as shown in Fig. 3. The mesh in the region around the airfoil is focused to capture the physics more accurately, as shown in Fig. 4. The used mesh in the analysis has 1.7 million nodes and 24,800 elements. Mesh cells are structured around in the airfoil vicinity to ensure that Y+ is in order of unity.

Three time steps are studied to stand on the most suitable one, where the plunging period is divided into 100, 200 and 400 steps per period. In this test, a nonsinusoidal waveform is used to ensure that the time discretization is robust enough the plunging waveform follows Eq. (8).

$$y(t) = A[0.8\sin(2\pi ft) + 0.2\sin(6\pi ft)]. \qquad (8)$$

As shown in Fig. 5, the three discretization steps produce identical results. Consequently, the 100 steps per cycle is to be used hereafter.

In order to validate the present setup, a benchmark case is simulated and compared to Young and Lai [18]. In this case, the reduced frequency is 4 and the nondimensional plunge amplitude is 0.15, and Reynolds number is 20,000. By comparing the present setup with [18], the results show good agreement as shown in Fig. 6, where the error in lift and thrust coefficients are 1% and 2% in the mean values, respectively.

3. Results

3.1. *Flow field behavior*

The flow field behavior is studied in terms of the vortex structure created by the proposed waveform for different

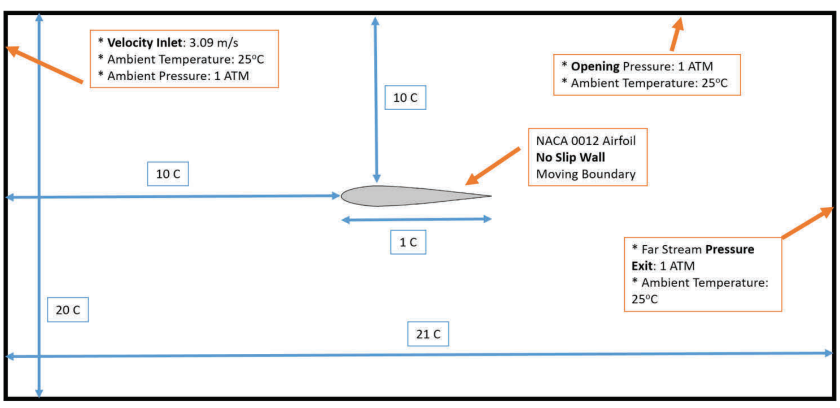

Fig. 3. The computational domain showing the dimensions and the boundary conditions.

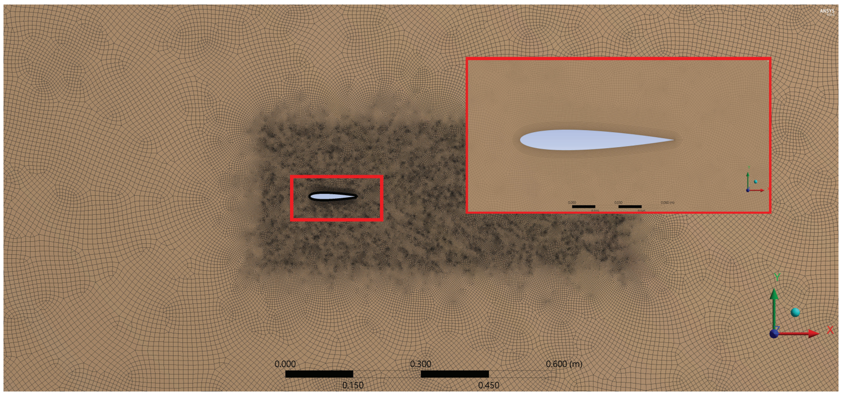

Fig. 4. Computational domain and grid.

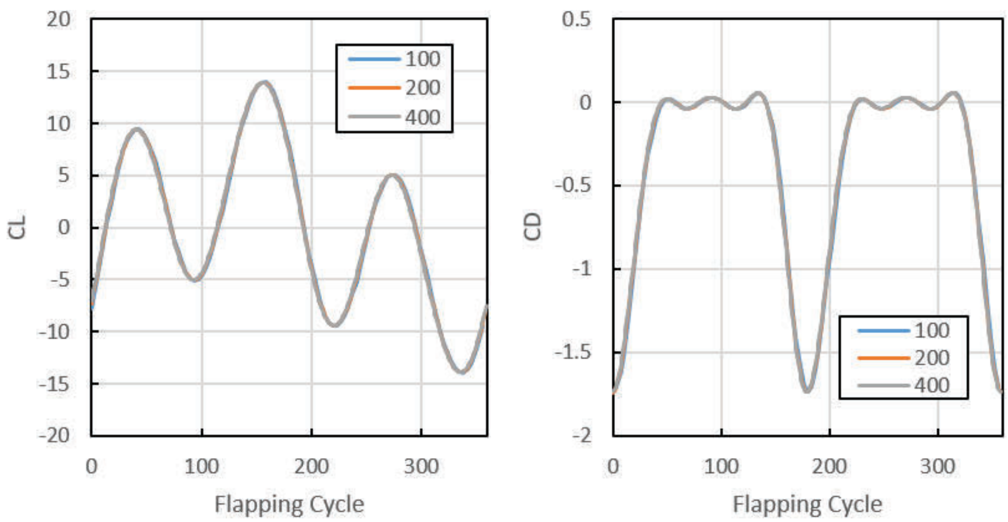

(a) (b)

Fig. 5. Variation of (a) lift and (b) drag coefficients with time steps per cycle.

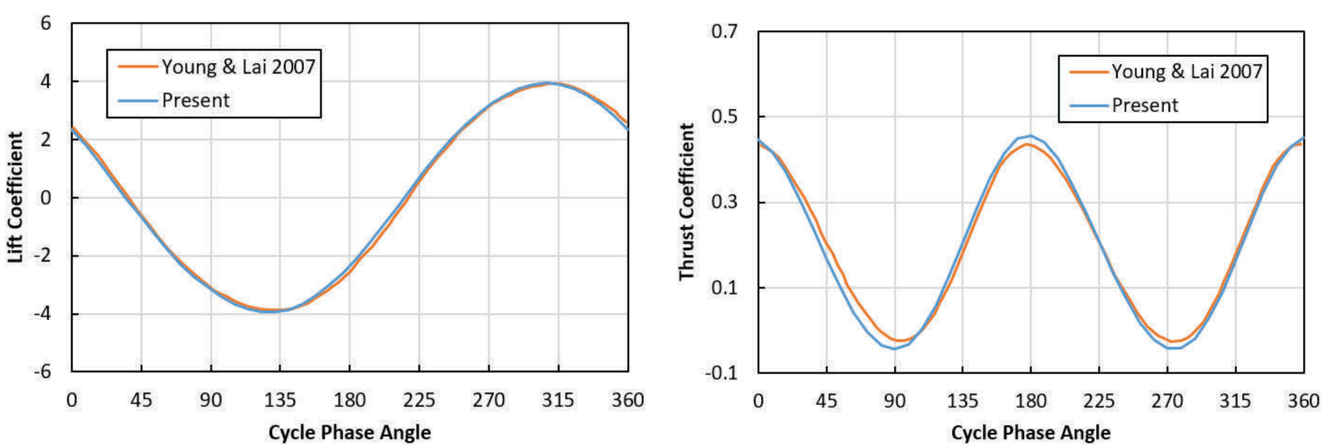

(a) (b)

Fig. 6. Validation of (a) lift and (b) drag coefficients variation with flapping cycle compared to Young and Lai [18].

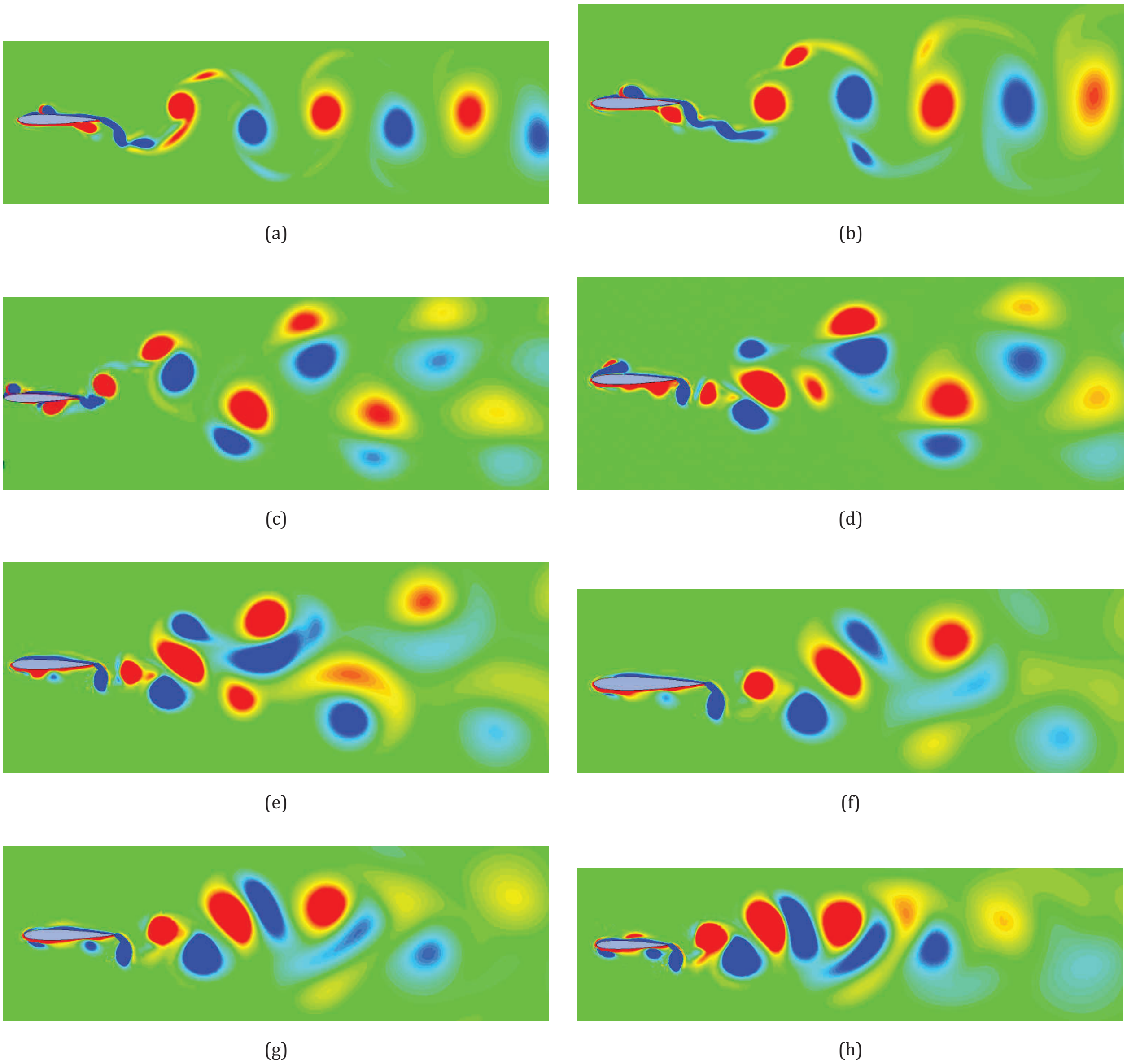

Fig. 7. Vorticity contours for the sinusoidal waves superposition waveforms at different weighting factors, (a) $\alpha = 1$, (b) $\alpha = 0.9$, (c) $\alpha = 0.8$, (d) $\alpha = 0.7$, (e) $\alpha = 0.6$, (f) $\alpha = 0.5$, (g) $\alpha = 0.4$ and (h) $\alpha = 0.3$.

values of the weighting factor, as shown in Fig. 7. The regular pattern of reverse von Karman sheet appears clearly in case of $\alpha = 1.0$. Then, for $\alpha = 0.9$ a small vortex appears close to the main vortex sheet, known as 2Po structure, and decays quickly downstream. Further reduction in α, reaching 0.8, the vortices become organized in pairs (2P structure [19] nomenclature). By further reduction in α small vortices appear close to the vortex pairs (dipoles) ($\alpha = 0.7$), then these vortices intensify and merge with the dipoles ($\alpha = 0.6$) making a concave vortex surrounding an opposite-signed vortex. Starting from $\alpha = 0.5$ the concave cortex deforms to look like *V* shape surrounding the opposite-signed vortex. This pattern is preserved until $\alpha = 0.3$, except for the vortices become closer to each other.

3.2. *Instantaneous aerodynamic coefficients*

Four parameters are considered hereafter, namely, lift, drag/thrust, friction and power coefficients, as shown in Figs. 8–11. The drag coefficient has six peaks, symmetric around the period center (angle of 180°), where the peak amplitude is inversely proportional to α. In other words, the further from sine, the more thrust achieved. The first peak shows a deviation as α decreases, leading to achieve

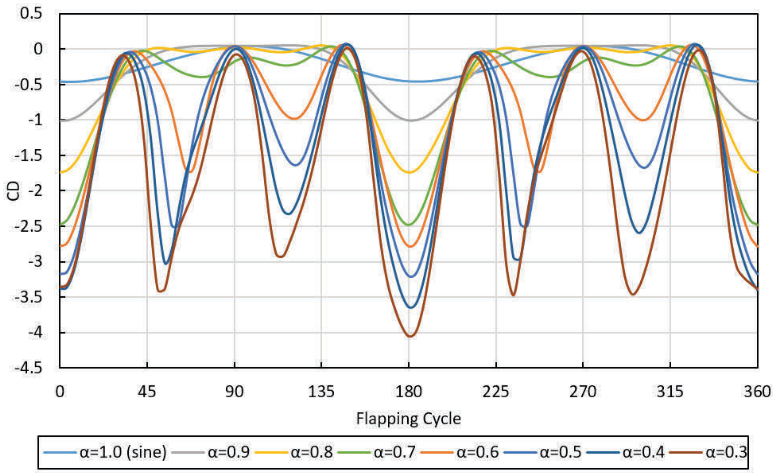

Fig. 8. The instantaneous drag coefficient for the proposed waveforms.

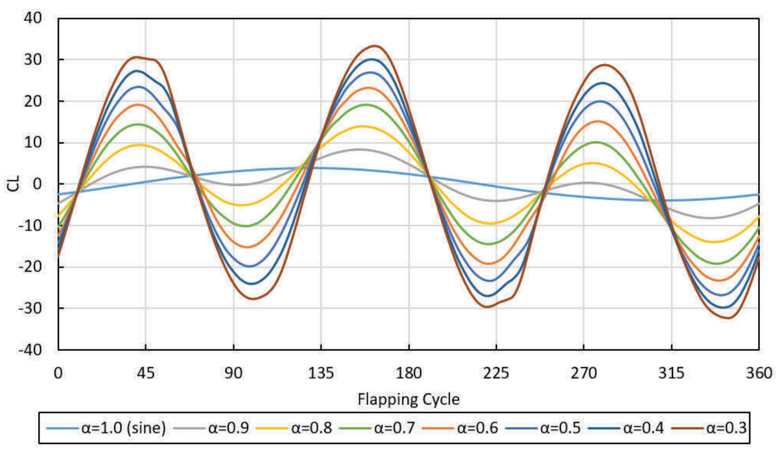

Fig. 9. The instantaneous lift coefficient for the proposed waveforms.

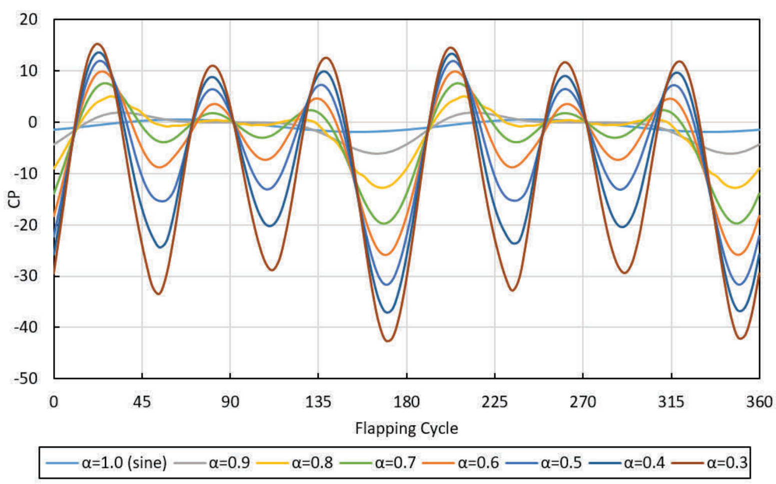

Fig. 10. The instantaneous power coefficient for the proposed waveforms.

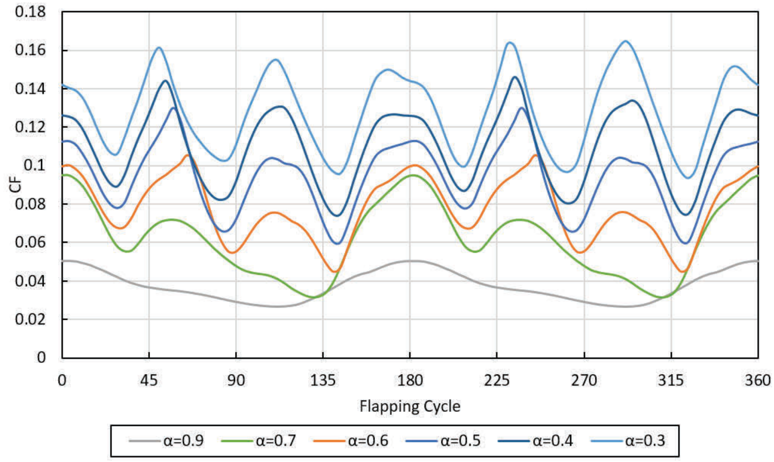

Fig. 11. The instantaneous friction drag coefficient for the proposed waveforms.

maximum instantaneous thrust earlier. Besides, the peaks in the vicinity of flapping angles 0° and 180° are much higher compared to the other peaks. This is due to the stronger TEV generated during the up-and downstroke.

The instantaneous lift coefficient shows six inflection points, with peaks inversely proportional to α. The first and fourth peaks show small kink at α of 0.5 and less, indicating some interactions related with the Leading Edge Vortices (LEVs).

The power coefficient shows 12 inflection points, the maximum ones are these in the vicinity of the flapping angle of 0° and 180°, as those of the drag coefficient. The peaks increase as the waveform moves apart of the regular sine waveform.

Considering friction drag, it shows similar behavior to the total drag coefficient in terms of number of peaks and the symmetry about the period center. Regarding its maximum value, it increases rapidly reaching 0.16 at $\alpha = 0.3$, compared to 0.05 in the regular sinusoidal case. Besides, the mean friction coefficient and the peaks of each case are distinct from each other, indicating the large effect of the weightings parameter α on the friction. This occurs because of intensifying the LEvs and TEVs around the airfoil. Yet, these suggestions shall be studied with further details.

3.3. *Mean aerodynamic coefficients*

The time-averaged aerodynamic and propulsive performance parameters are studied for the Sinusoidal Waves Superposition waveform, with variation of the weighting parameter α from 1.0 to 0.3. It is found that as α increases (the local minimum between the two peaks of the waveform close to the nondimensional times 0.25 and 0.75 in Fig. 1)

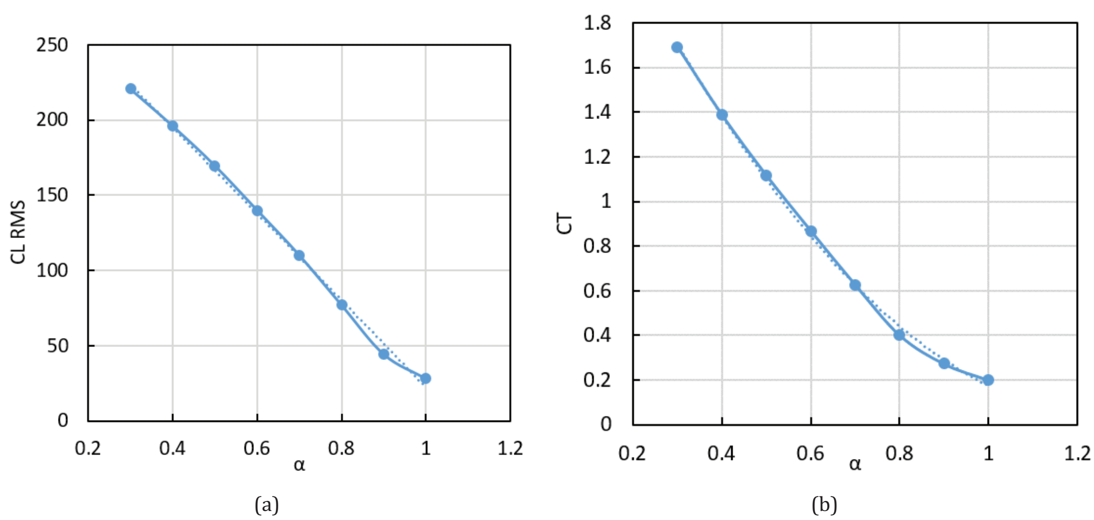

Fig. 12. Variation of the weighting parameter α and its effect on (a) lift, (b) thrust, (c) power and (d) propulsive efficiency. The dotted lines represent the regression model to depict its relative accuracy.

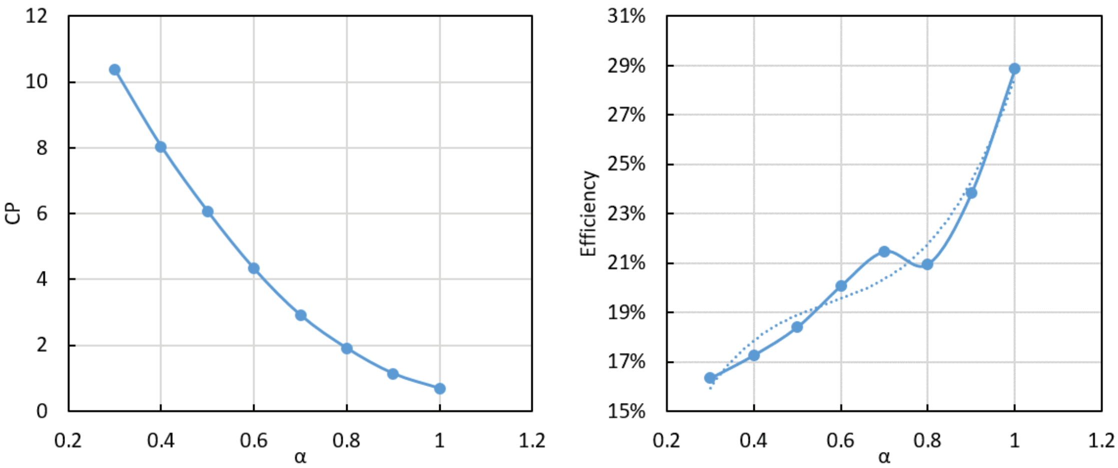

(c) (d)

Fig. 12. (*Continued*)

the airfoil is subjected to stronger lift forces, and produces higher thrust and more power is required. Yet, the rate of power than the increment in thrust, leading ultimately to reduction in propulsive efficiency, as shown in Fig. 12. One interesting point here is that this proposed waveform can increase the thrust by 135% with 5% reduction in efficiency, and 200% with reduction less than 8% in efficiency. This can help in designing a flapping drone with speed booster without much reduction in efficiency.

In this figure, the time averaging over the plunging period is used in thrust and power coefficients, while the Root Mean Squared (RMS) averaging is used for the lift coefficient. This is used because the airfoil is symmetric and the flow has no angle of attack, so the time average of the lift coefficient equals to zero. For such a reason, the RMS averaging is utilized, although it gives very high values, as shown in Fig. 12(a).

4. Linear Regression Modelling

Aim of developing a regression model is to allow the flight controller of the drone to estimate the required parameters for the desired performance instantaneously through one simple equation with minimum computational power. The fine tuning of the exact parameters is to be obtained later by whatever control law utilized by the flight controller. This will simplify the performance prediction of the FWUAV without any need to calculate each and every case of the present flapping waveform, so the flight controller can estimate the FWUAV performance in the real time using just one more equation. This will enhance the performance by enabling the flight controller to vary the flapping pattern according to the instantaneous situation during the flight.

This work models the behavior of plunging using the sinusoidal waves superposition waveform as a function of the weighting factor, α. This factor is to be controlled mechanically through a set of gears or a similar mechanism, but this is out of the scope of the present work. Using polynomial functions, it is found that the RMS lift (Eq. (9)), mean thrust (Eq. (10)) and power (Eq. (11)) coefficients and the propulsive efficiency (Eq. (12)) fit well and can create an accurate model as shown, with accuracy of 99.8%, 99.7%, 100% and 97.1%, respectively, based on $R2$ parameter.

$$C_{L,\mathrm{RMS}}(\alpha) = 1.7132 \times \alpha^2 - 4.4179 \times \alpha + 2.8785, \quad (9)$$

$$C_T(\alpha) = -5.9943 \times \alpha^2 - 279.73 \times \alpha + 307.78, \quad (10)$$

$$C_P(\alpha) = 15.707 \times \alpha^2 - 34.223 \times \alpha + 19.216, \quad (11)$$

$$\eta_{\mathrm{prop}}(\alpha) = 0.8302 \times \alpha^3 - 1.4304 \times \alpha^2 + 0.8847\alpha + 0.0004. \quad (12)$$

The propulsive efficiency has the minimum accuracy as expected because it is the ratio between thrust and power coefficients as shown in Eq. (7). If the models of the thrust and power coefficients are divided, then a more accurate model can be obtained for the propulsive efficiency. Yet, this model is not considered here because it takes more computational time.

5. Summary and Conclusion

The aerodynamic and propulsive performance of Sinusoidal Waves Superposition plunging waveform is studied. This proposed waveform creates additional trailing edge vortices and control their strength. This is realized by super-positioning between the main sinusoidal wave and a three-times faster sinusoidal one and weighted by the parameter α. The performance parameters are quantified in terms of lift, drag, thrust, power coefficients and the propulsive efficiency. Both time-dependent and time-averaged performance are studied, and the wake pattern is depicted.

Regarding the time-averaged performance, as the additional trailing edge vortices intensify, the lift, thrust and power coefficients increase without much effect occurs in the propulsive efficiency. Quantitatively speaking, 135% and 200% increment in thrust can occur with reduction less than 5% and 8% in efficiency, which can lead to manufacturing a flapping drone with speed booster without considerable penalty in efficiency.

Regression modeling for the aerodynamic and propulsive efficiency is conducted to estimate them based on the weight of the faster wave. The regression model is studied to enable the flight controller to estimate the required parameters for the required performance instantaneously with minimum computational power. Accuracy of 97% is achieved.

ORCID

Mostafa El-Salamony https://orcid.org/0000-0003-2360-052X

References

[1] L. Ilieva, I. Ursano, L. Traista, B. Hoffmann and H. Dahy, Biomimicry as a sustainable design methodologyintroducing the 'biomimicry for sustainability' framework, *Biomimetics* **7** (2022) 37.

[2] J. Zhang, N. Zhao and F. Qu, Bio-inspired flapping wing robots with foldable or deformable wings: A review, *Bioinspir. Biomim.* **18** (2022) 011.

[3] J. Young, J. C. S. Lai and M. F. Platzer, A review of progress and challenges in flapping foil power generation, *Progress Aerospace Sci.* **67** (2014) 2–28.

[4] Z. Terze, V. Pandza, M. Kasalo and D. Zlatar, Discrete mechanics and optimal control optimization of flapping wing dynamics for mars exploration, *Aerospace Sci. Technol.* **106** (2020) 106131.

[5] K. Telli, O. Kraa, Y. Himeur, A. Ouamane, M. Boumehraz, S. Atalla and W. Mansoor, A comprehensive review of recent research trends on UAVs, preprint (2023), arXiv:abs/2307.13691.

[6] H. E. Taha, M. R. Hajj and A. H. Nayfeh, Flight dynamics and control of flapping-wing mavs: A review, *Nonlinear Dyn.* **70** (2012) 907–939.

[7] X. Fang, Y. Wen, Z. Gao, K. Gao, Q. Luo, H. Peng and R. Du, Review of the flight control method of a bird-like flapping-wing air vehicle, *Micromachines* **14** (2023) 1547.

[8] C. Lee, S.-B. Kim and B. Chu, A survey: Flight mechanism and mechanical structure of the UAV, *Int. J. Precision Eng. Manufactur.* **22** (2021) 719–743.

[9] M. F. B. Abas, A. S. M. Rafie, H. Yusoff and K. A. Ahmad, Flapping wing micro-aerial-vehicle: Kinematics, membranes, and flapping mechanisms of ornithopter and insect flight, *Chin. J. Aeronautics* **29** (2016) 1159–1177.

[10] S. Ryu, J. G. Lee and H. Kim, Design, fabrication, and analysis of flapping and folding wing mechanism for a robotic bird, *J. Bionic Eng.* **17** (2020) 229–240.

[11] E. F. Helbling and R. J. Wood, A review of propulsion, power, and control architectures for insect-scale flapping-wing vehicles, *Appl. Mech. Rev.* **70** (2018) 010801.

[12] A. Boudis, H. Oualli, A. Benzaoui, O. Guerri, A.-C. Bayeul-Lainé and O. Coutier-Delgosha, Effects of non-sinusoidal motion and effective angle of attack on energy extraction performance of a fully-activated flapping foil, *J. Appl. Fluid Mech.* **14** (2021) 485–498.

[13] A. Boudis, A.-C. Bayeul-Lainé, A. Benzaoui, H. Oualli, O. Guerri and O. Coutier-Delgosha, Numerical investigation of the effects of non-sinusoidal motion trajectory on the propulsion mechanismsof a flapping airfoil, *J. Fluids Eng.* **141** (2019) 041106.

[14] Z. Qi, J. Zhai, G. Li and J. Peng, Effects of non-sinusoidal pitching motion on the propulsion performance of an oscillating foil, *PLoS One* **14** (2019) e0218832.

[15] M. El-Salamony, On plunging using double-peak kinematics, *Phys. Fluids* **36**(10) (2024).

[16] X. Wu, X. Zhang, X. Tian, X. Li and W. Lu, A review on fluid dynamics of flapping foils, *Ocean Eng.* **195** (2020) 106712.

[17] J. D. Eldredge and A. R. Jones, Leading-edge vortices: Mechanics and modeling, *Ann. Rev. Fluid Mech.* **51** (2019) 75–104.

[18] J. Young and J. C. S. Lai, On the aerodynamic forces of a plunging airfoil, *J. Mech. Sci. Technol.* **21** (2007) 1388–1397.

[19] M. M. Koochesfahani, Vortical patterns in the wake of an oscillating airfoil, *AIAA J.* **27** (1987) 1200–1205.

Mostafa El-Salamony is a PhD Candidate at Peking University, China, in the field of flapping aerodynamics. He studied his M.Sc. at Moscow Institute of Physics and Technology, Russia, and B.Sc. at Institute of Aviation Engineering and Technology, Egypt. His research interests include drones and aircraft design, machine learning in aerospace, and high-speed aerodynamics and boundary layer stability.